Available online at www.sciencedirect.com
SCIENCE DIRECT®
PERGAMON
International Journal of Heat and Mass Transfer 46 (2003) 4179–4189
International Journal of HEAT and MASS TRANSFER
www.elsevier.com/locate/ijhmt

The effects of the number and angle of microgrooves on the liquid film in horizontal annular two-phase flow

Timothy A. Shedd [a,*], Ty A. Newell [b], Pei Keow Lee [b]

[a] *Department of Mechanical Engineering, University of Wisconsin—Madison, 1500 Engineering Drive, Madison, WI 53706, USA*

[b] *Department of Mechanical and Industrial Engineering, University of Illinois at Urbana–Champaign, 1206 W. Green Street, Urbana, IL 61801, USA*

Received 12 September 2001; received in revised form 28 April 2003

Abstract

Measurements of the liquid film profile and pressure drop were made in tubes with grooves of varying angle (0°, 9° and 18°) as well as tubes with varying numbers of grooves at a common angle (18°). These data indicate that the grooves act to redistribute the liquid film on the inner wall perimeter and that only a relatively small number of grooves (12) is needed to do this. The grooves also affect the stability of the vapor–liquid interface and can generate lower average liquid film thickness. The pressure loss is directly related to the number of grooves for the tubes studied.

1. Introduction

Micro-fin tubes have become important components of modern air conditioning and refrigeration systems with their significantly enhanced heat transfer coefficients and low pressure loss characteristics. Though a substantial amount of data has been gathered and generalized predictive correlations have been generated with some success, a fundamental understanding of the two-phase vapor–liquid flow behavior through these tubes is still lacking. In this work, detailed measurements of the liquid film distribution during the annular flow regime have been performed using a non-intrusive optical technique. Experimental work detailed in Shedd [1] demonstrated that the grooves act to promote the transition from stratified to annular flow at lower qualities and/or liquid flow rates. In addition, it was noted that the steady-state film profiles tend to show a rotated symmetry; the thinnest and thickest parts of the film tend to occur at locations shifted from the top or bottom center in the direction of the groove rotation. This work describes the efforts to determine how the groove angle and the number of grooves affect the redistribution of the liquid film in annular flow.

2. Background

In one of the earliest studies to specifically address groove angle, Ito and Kimura [2], tested aluminum tubes with 0° (axial), 3°, 7°, 15°, 30°, and 75° grooves under varying mass and heat flux conditions and an average quality of about 0.6, though the inlet and outlet qualities were not given. They noted a maximum at the low angles (between 7° and 15°) and a subsequent decrease in performance as angle increased. This is corroborated in a later study performed by Oh and Bergles [3]. At a lower mass flux (50 kg/m^2 s), however, Oh and Bergles found that the best performing angle shifted higher to around 18°, with larger angles generally performing better than those below 12°. This trend is shown in the data of Kimura and Ito [4] and Yoshida et al. [5] as well.

The work of Kimura and Ito [4] and Chamra et al. [6] shows that evaporation performance at a mass flux from about 100 to 200 kg/m^2 s has a broad peak in tubes with angles ranging from about 18° to 25°.

Averaged heat transfer coefficients obtained by Khanpara et al. [7] and Schlager et al. [8,9] for tubes

* Corresponding author. Fax: +1-608-262-8464.
E-mail address: shedd@engr.wisc.edu (T.A. Shedd).

0017-9310/$ - see front matter © 2003 Elsevier Ltd. All rights reserved.
doi:10.1016/S0017-9310(03)00250-3

Nomenclature

d	diameter of the tube
Ft	Froude rate parameter, Eq. (1)
g	acceleration due to gravity
G	mass flux (kg/sm^2)
$\dot{m}_g$	mass flow rate of vapor (kg/s)
$\dot{m}_l$	mass flow rate of liquid (kg/s)
n	number of grooves
U_{sg}	superficial velocity of vapor
x	mass quality
X_{tt}	Lockhart-Martinelli parameter, Eq. (7)

Greek symbols

γ	film rotation angle
Υ	film uniformity, Eq. (3)

with varying fin heights and shapes show that, in general, evaporation enhancement improves as the angle increases. The Schlager et al. data generally show the opposite trend for condensation, but this effect may be due to the variation in groove depth between the tubes. Condensation heat transfer is rather sensitive to groove depth due to the effects of surface tension on the film coating fins. Indeed, Chamra et al. [10] show the condensation heat transfer coefficient consistently to increase with fin angle.

Groove depth seemed to effect the pressure drop data of Schlager et al. as well. Groove depth appeared to be a greater factor than groove angle for a 9.52 mm tube. Flows through a 12.7 mm tube behaved differently, with pressure drop proportional to groove angle, possibly because the groove depth relative to the diameter became less significant. In the data of Chamra et al., pressure drop in both condensation and evaporation rose linearly with groove angle. The small variation in groove number did not appear to influence either the heat transfer or pressure drop data.

Comparison of the performance of tubes with axial (0° helix) grooves to those with helical grooves is particularly interesting. Ito and Kimura [2] found the performance of the axial tubes to be worse than any helical tube at all conditions tested in evaporation. Chiang [11], on the other hand, tested condensation and evaporation at high mass flux and found that the axial tubes outperformed the helical at all flow and heat flux conditions but the lowest mass flux in evaporation. This difference may be explained completely or in part by the large differences in the geometries of the fins used in the axial and helical tubes tested. The helical tubes had fewer fins and a broader apex angle (40–50° versus 15°). The patent by Shinohara et al. [12] documents that a tube with fins having 15° apex angles will outperform fins with 45° apex angles by almost 50% in both evaporation and condensation.

To address this geometrical discrepancy, Graham et al. [13] undertook an experiment to compare the condensation performance of tubes with helical and axial fins of nearly identical geometries. They found that the axial tube outperformed the helical at mass flux conditions of 150 kg/m^2 s and higher. The enhancement over the smooth tube was quality-dependent, however. When a simple flow regime indicator, the Froude rate, was applied to the data, it became apparent that the axial grooves appeared to maintain an annular flow condition to lower qualities than did a smooth or the helical tube.

Applying the same indicator to the Ito et al. data, it is seen that the poor axial performance around a quality of 0.6 may be due to the axial grooves delaying a transition to annular flow, or impeding the wetting of the tube wall by waves.

Less information has been published on the relationship between pressure loss and groove angle. Ito and Kimura, found that, for single phase flow, tubes with fins at 15° or less generated only slightly larger pressure drops than smooth tubes. Fins at 30° presented noticeable resistance, while the pressure drop increased to about 1.5 times the smooth tube at 45°, about 2 times at 75° and about 2.5 times at 90°. Two-phase pressure drops were measured by Chamra et al. [6,10] for 15–27° fin angles and found to increase in a fairly linear manner with angle in both evaporation and condensation.

3. Experiment

The flow conditions examined are shown in Table 1. The Froude rate, Ft, is a non-dimensional group that essentially represents the ratio of the rate of kinetic en-

Table 1
Details of the experimental flow conditions

Name	$\dot{m}_g$, kg/s	$\dot{m}_l$, kg/s	Ft	x	G, kg/m^2 s
T	0.0048	0.0032	70	0.6	44
U	0.0067	0.0032	120	0.68	55
V	0.0099	0.0032	210	0.76	73
Q	0.0047	0.0063	50	0.42	61
R	0.0079	0.0063	105	0.56	79
F	0.0110	0.0063	165	0.64	97
G	0.0152	0.0063	250	0.71	120

Ft is the Froude rate, x is quality and G is mass flux. See text for an explanation of the Froude rate parameter.

ergy flowing in the vapor to the power required to pump liquid from the bottom to the top of the tube at its axial flow rate. It is defined by

$$\mathrm{Ft} = \left(\frac{\dot{m}_g}{\dot{m}_l}\right)^{0.5} \mathrm{Fr} = \left(\frac{\dot{m}_g}{\dot{m}_l}\right)^{0.5} \left(\frac{U_{sg}}{(gd)^{0.5}}\right) \quad (1)$$

where the subscripts 'g' and 'l' represent vapor and liquid quantities, respectively, U_{sg} is the superficial vapor velocity (the velocity of vapor if it occupied the entire tube at the same mass flow rate), g is the gravitational acceleration and d is the tube diameter.

The test sections were constructed of 15.1 mm inner diameter clear PVC tubing. Approximately 200 micron deep grooves were created on the inside wall of the plastic tube by a scribing process. The total observable length was about 6 m including a 3 m smooth flow development section. Three different tubes with 20 grooves were fabricated with angles of 0°, 9° and 18°. Three additional 18° helix tubes were made in the same manner with 4, 8 and 12 grooves.

Laboratory compressed air was regulated and passed through a 3 m entrance tube. The mass flow rate of the air was determined by measuring the pressure drop across this entrance tube. The Colebrook correlation for friction factor, along with the definitions of friction factor, Reynolds number and mass flow rate, were then solved simultaneously to provide the mass flow rate of air in the loop. A propagation of error analysis performed for this experiment according to Taylor and Kuyatt [14] gives a total worst-case uncertainty of 3.5% in the air mass flow measurement. Water from the laboratory main passed through a bank of volumetric flow meters before entering the test section through several 1.6 mm holes drilled in the test section wall. Experimental uncertainties were ±5% based on manufacturer's data. Both the water and air were filtered to 5 microns prior to entering the apparatus.

Pressure gradients were measured using solid state differential pressure transducers. The inlet pressure transducer had a sensitivity of ±1.7 Pa while the test section transducers were sensitive to ±6.8 Pa. Gauge pressures in the entrance and test sections were monitored with Bourdon-tube gauges.

Local liquid film thicknesses were obtained using an optical measurement system described by Shedd and Newell [15]. The time averaged liquid film thicknesses presented here were measured to within ±0.003 mm (± one standard error). As has been verified by Plzak and Shedd [16], the experimental results presented here exclude large liquid waves from the calculated average thickness; the thicknesses reported reflect only the thin base film that exists between the large liquid waves. This is significant since it is this thin base film that apparently plays the most active role in heat transfer [17]. The film thicknesses were measured at about 390 L/D from the point where liquid was introduced.

4. Results

4.1. Influence of the helix angle on the liquid film profiles

Figs. 1 and 2 show a direct comparison of the film profiles for four of the seven flow conditions in the 0°, 9° and 18° helix tubes, all with 20 grooves. The most striking behavior for the 9° and 18° helix tubes is the film rotation. The thinnest and thickest regions of these films appear to be rotated from the top and bottom center locations, respectively. From casual inspection, it is not clear which of the 9° or 18° helix rotate the film more.

The 0°, or axially grooved, tube behaves differently than the other two. Most noticeable are the regions on the sides of the tube where a stable, thicker film appears to form. These may be indications that forces pushing liquid up the wall meet resistance in the grooves and these locations reflect the equilibrium reached between the upward forces and gravity in the presence of the horizontal grooves. The rivulet at the top of the axial tube in Flow T (Fig. 1) reflects the observed behavior that droplets landing on the upper surfaces of the axial tube tend to "stick" and combine to form rivulets flowing along the grooves. This could be a mechanism of enhanced wetting and film formation for the axial tubes in conditions where entrainment of liquid droplets is significant.

4.2. Influence of the number of grooves on the liquid film profiles

The film profiles in the 4, 8, 12 and 20 groove 18° helix tubes for Flows T, V, Q and F are presented in Figs. 3 and 4. The remaining film profiles, along with tables of the local film thickness values, can be found in Shedd [1]. Though the profiles contain irregularities, the effect of increasing the number of grooves is readily apparent. In Flow Q, for instance, the thinnest and thickest parts of the film are not significantly offset from the smooth tube film for the 4 groove tube. As the number of grooves increases, an increasing amount of liquid appears to be drawn from the left side to the right side of the tube. Thus, the degree of rotation of the film profile appears to be directly related to the number of grooves, at least for these low numbers.

4.3. Quantifying the film rotation

It is apparent from the plots of the film profiles in the tube with helical grooves that the film appears to have been rotated; i.e. the thinnest and thickest parts of the film appear to have been shifted counterclockwise from

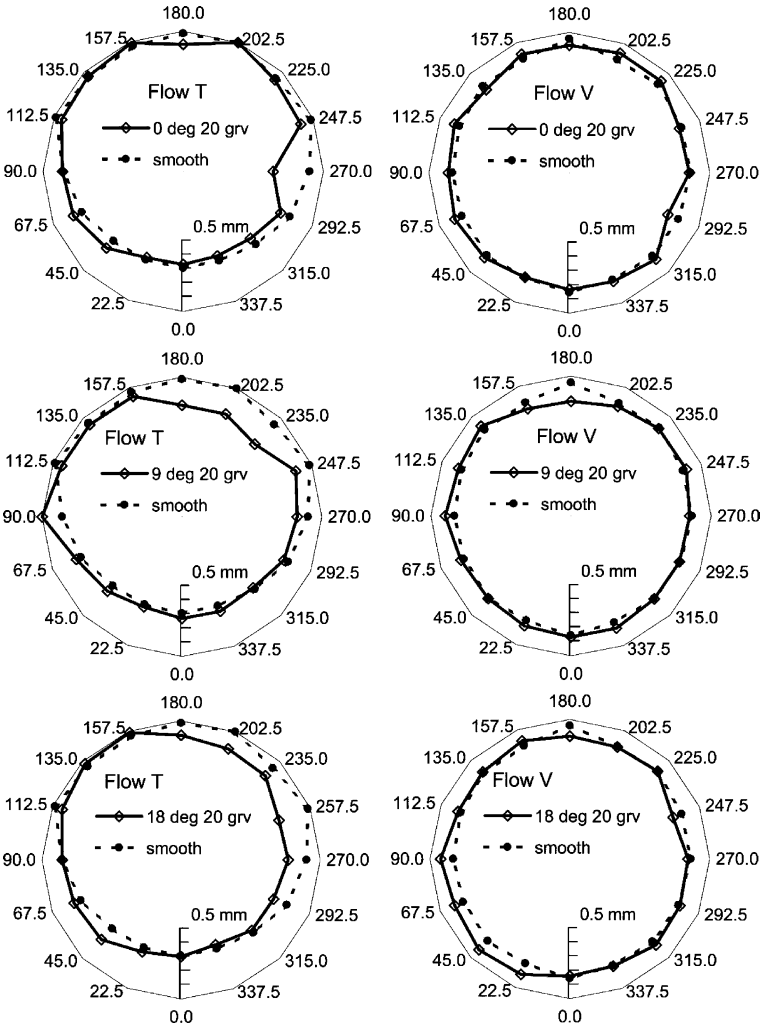

Fig. 1. Film thickness profiles in the 0°, 9° and 18° helix tubes for Flows T and V.

the top and bottom center locations, respectively. Manual approximations of the angle through which the film was rotated proved to be very difficult and inconsistent, however. As a means of quantifying the rotation, a cross-correlation scheme was developed whereby an "ideal" film was rotated on top of the experimental data and the angle at which the highest correlation resulted was defined as the rotation angle of the film. The ideal film was a circle representing a uniform annular film that was then shifted upward slightly with respect to the tube wall. Initially placed at 0°, the values of this eccentric circle at each of the data locations (every 22.5°) was multiplied with the data and the sum of these products was found. The eccentric circle was then rotated 0.5° and the process was repeated through 359.5°.

The resulting correlation data contained a minimum and a maximum which, if the experimental data were truly a rotated form of the symmetrical smooth tube profile, would be separated by 180°. In practice, the separation was between 175° and 185°. As a general observation, flows with markedly thicker films on the bottom, such as T and Q, show less of a rotation within the thicker region than in the thinner region, thus leading to a greater separation between the angles of rotation at the maximum and minimum film locations. The final definition of the film rotation angle was the average of the angles through which the minimum and maximum were rotated from their center positions.

Counterclockwise rotation was defined to be positive in agreement with the direction of the helical grooves in the tube.

This method appeared to be very effective and produced results that seemed to agree with visual inspection of the plots. However the determination of the angle of

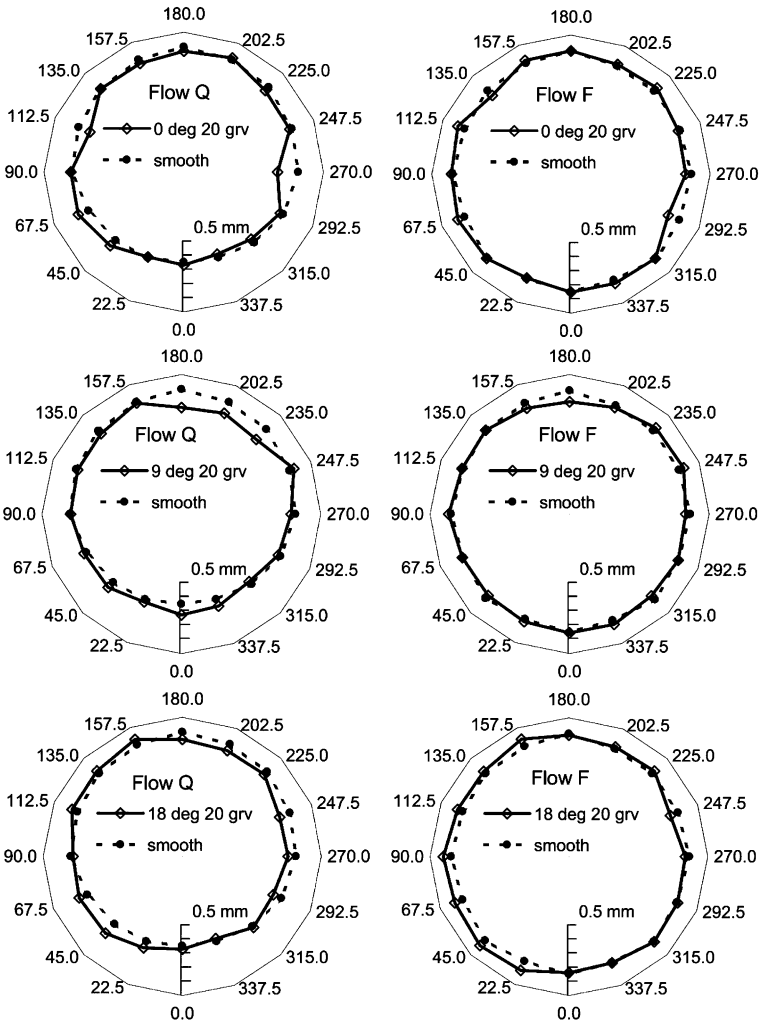

Fig. 2. Film thickness profiles in the 0°, 9° and 18° helix tubes for Flows Q and F.

rotation of the more uniform films was quite sensitive to small variations in thickness. For example, a change of 0.01 mm at one location of a Flow G profile could change the rotation by 10° or more.

4.4. Rotation of the film and the groove helix angle

Fig. 5a shows how the film rotation angle, γ, determined by the cross-correlation method just described, varies with tube helix angle for each of the flows. At each helix angle, the film rotation is generally proportional to the vapor velocity. No clear trends are evident from this data as to the relation of helix angle to film rotation. Inspection of the film profile plots will confirm that the large rotation angles of the 9° data appear to be physically reasonable. Incomplete film thickness data obtained for flows F and G at a location one meter upstream from the data presented here give a somewhat lower, non-inverted rotation angle. This suggests that a steady state film profile may be obtained that varies along the tube length. More data are needed to confirm this. However, it should be noted that the data presented in this study were very repeatable within the experimental uncertainty, including the apparent inversion of the film thickness.

An interesting observation from this plot is that the smooth tube data were never perfectly symmetrical with the vertical. The negative rotation angle indicates that the films were rotated clockwise with respect to a vertically symmetric film. It is possible that the magnitude of the very large rotations for Flows F and G (−32° and −61°, respectively) are not the true film rotations due to the sensitivity of the correlation method

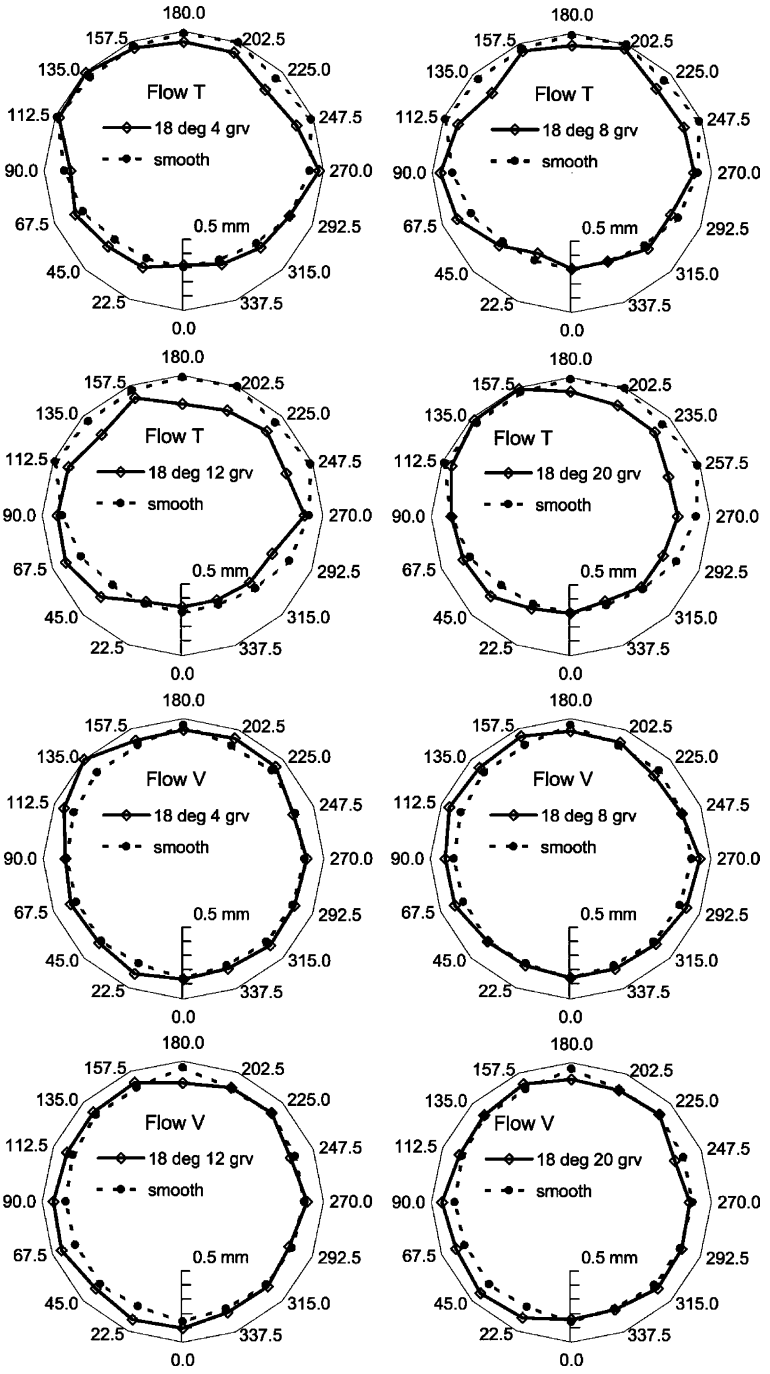

Fig. 3. Film thickness profiles in tubes with 4, 8, 12 and 20 18° helix grooves for Flows T and V.

when applied to these relatively uniform films. However, close inspection of the plots and film thickness data indicate that, indeed, the axis of vertical symmetry in the film has been rotated, and that changes of the film thickness on the order of the standard error (about 0.003 mm) would have little effect on the profiles or the symmetry.

There is no reason to suspect that an annular film would tend to have a clockwise rotation in general. It is likely that this rotation is related to small variations in the

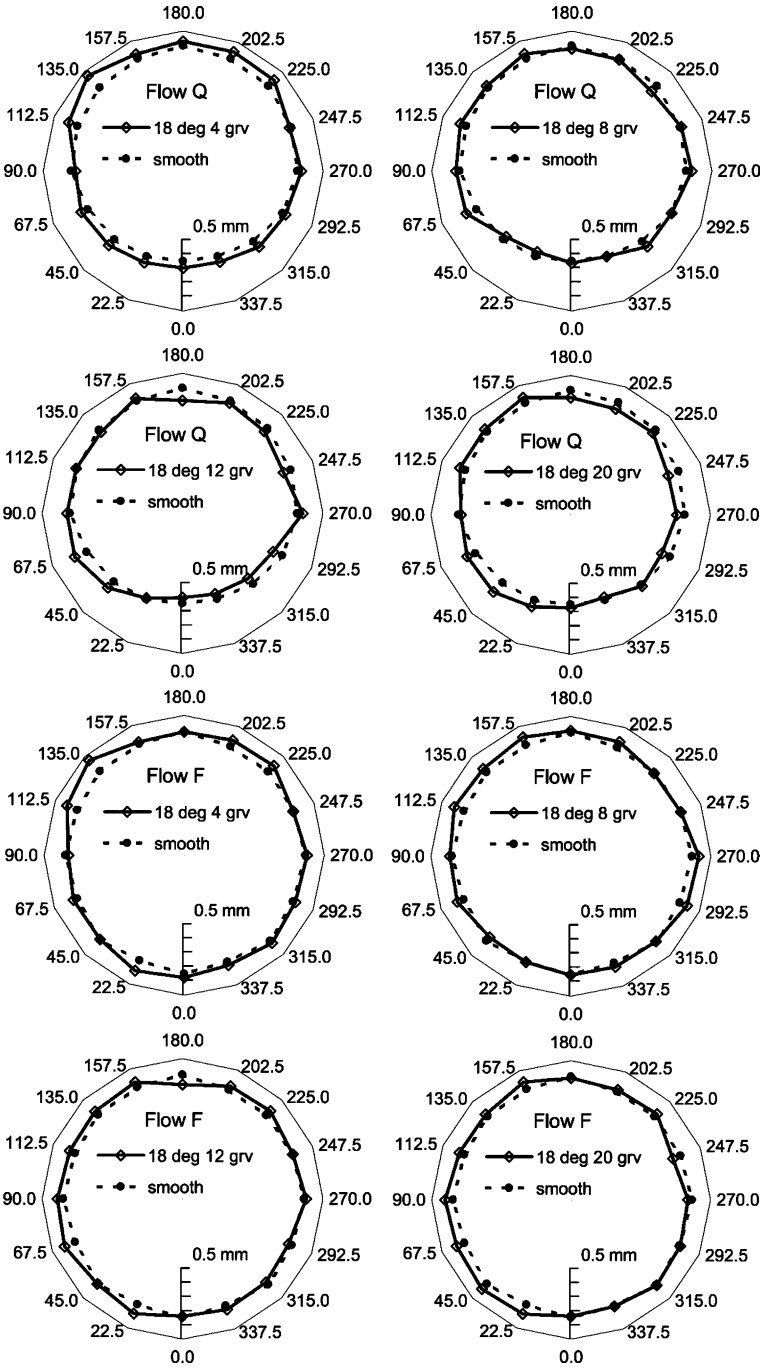

Fig. 4. Film thickness profiles in tubes with 4, 8, 12 and 20 18° helix grooves for Flows Q and F.

vapor and liquid flow induced by the particular orientation and construction of the flow loop. While it is usually assumed that the liquid film in annular flow through smooth tubes drains under the influence of gravity in a symmetrical manner down either side, a small variation in the flow could cause the film to preferentially drain to one side or the other. Thus, while it is almost universally assumed that the liquid film profiles in horizontal smooth tubes are vertically symmetrical it appears that, in fact, this may be the exception rather than the rule.

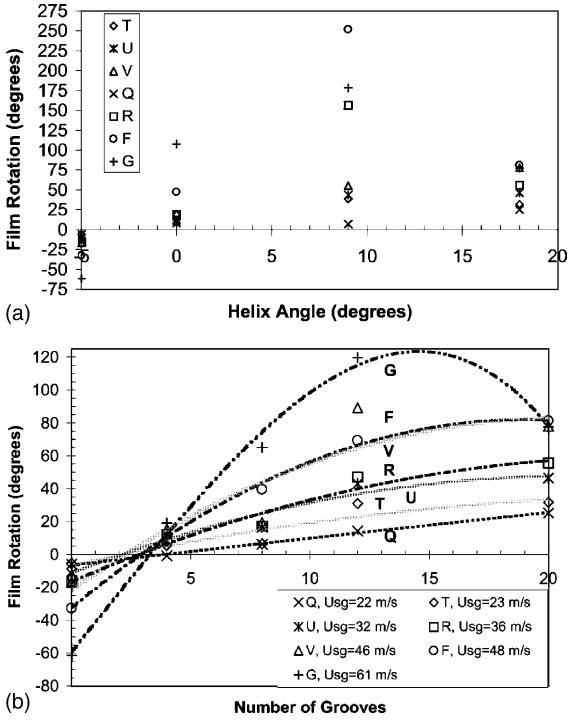

Fig. 5. (a) Film rotation versus helix angle and (b) film rotation versus number of 18° helical grooves. Positive rotation angle indicates a counterclockwise rotation. The data on the Y-axis represent the smooth tube film rotation. Patterned lines are polynomial curve fits of the raw data to better bring out trends.

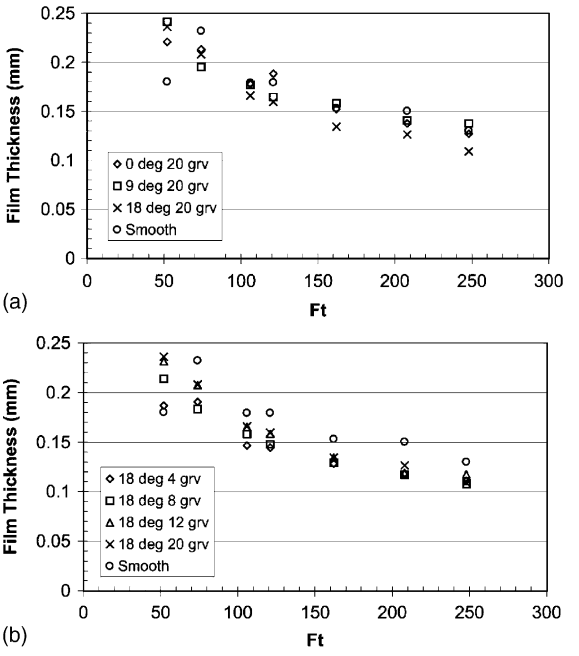

Fig. 6. Average film thickness over the wetted perimeter plotted against Froude rate with (a) groove angle and (b) number of grooves as parameters.

4.5. Film thickness and the groove helix angle

The relation of the groove helix angle to the average film thickness over the wetted tube perimeter is shown in Fig. 6a. It is interesting to note that, except at the lowest Froude rates (50, 70; Flows T and Q, the most asymmetrical flows), the 18° helix tube consistently has a lower average film thickness. The absolute differences in film thickness between the smooth and the 18° tube are on the order of 0.030 mm for the upper four flows, a difference of about 20%. This is also significantly greater than the standard error for the measurements.

Visual observation of the flow did not indicate any significant difference in behavior between the 18° tube and the others, other than the increased wetting of the walls. However, the 9°, and to some extent, the 0°, tubes showed increased wetting as well, yet the average film thickness did not fall as far in those tubes.

Since the film thickness was measured using light reflected from the surface, fluctuations in the surface of the liquid will cause variations in the reflection. Hence, the standard error of the film thickness measurements provide some indication as to the waviness of the liquid surface.

Two interesting trends are apparent in the film thickness standard error data (see [1] for detailed results). First, the general level of standard error rises with angle from the smooth to the 0°, 9°, and 18° tubes. This trend generally coincides with the thinner average film results reported in Fig. 6a. Thus, it appears possible that additional liquid mass is being carried by wave structures, leaving behind less film in the base layer. In addition, the error level was found to rise for thinner films as the angle increases for the 9° and 18° tubes while the error level appears nearly constant for the 0° tube across the span of film thickness. This possibly indicates that waves become more uniformly distributed around the tube, or at least that their characteristics become circumferentially more uniform.

As a means of quantifying the redistribution of liquid by the grooves, a film distribution parameter is defined as the film uniformity, Υ, multiplied by the wetted percentage of the tube wall perimeter, P,

$$\text{Dist} = \frac{P_{\text{wet}}}{P}\Upsilon. \tag{2}$$

The film uniformity, a measure of how uniformly the liquid is distributed over the wetted perimeter, is defined by

$$\text{Film uniformity} = 1 - \frac{\text{Standard deviation of film thickness measurements}}{\text{mean film thickness}}$$
$$\Upsilon = 1 - \frac{\sigma(h)}{\bar{h}}\bigg|_{\text{Wetted perimeter}}. \tag{3}$$

The film distribution parameter is plotted against mass quality in Fig. 7a with groove helix angle as a parameter. The 9° tube tended to show consistently better distribution across all flow conditions than any of the other tubes, although the 18° tube consistently had the thinnest average film thickness. Of particular interest is the observation that the smooth tube performs significantly worse than the grooved tubes at the lowest quality condition for each liquid mass flow. This is consistent with heat transfer data showing that grooved tubes show greatest enhancement over smooth at lower qualities and mass flux. This is apparently due to the increased wetting of the wall by the action of the grooves and somewhat increased uniformity. At higher qualities where the smooth tube annular film becomes more uniform, the heat transfer enhancement diminishes significantly and a similar trend could be inferred from the film distribution data presented here.

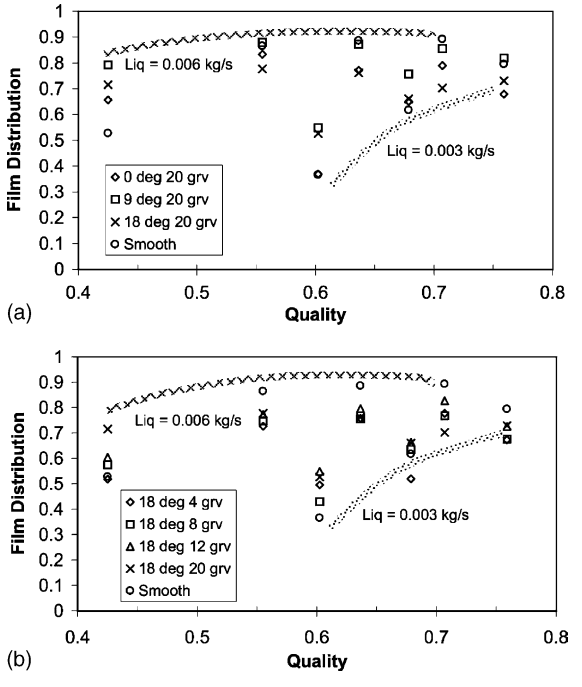

Fig. 7. Film distribution versus mass quality with (a) groove helix angle and (b) number of grooves as a parameter. Thick lines highlight groupings of data by liquid mass flow rate.

4.6. Film rotation and the number of grooves

When the angle of film rotation is plotted against the number of grooves in the tube for the same helix angle (18°s), some basic behaviors become apparent, as shown in Fig. 5a. Generally, the rotation angle increases with number of grooves. It is not clear why a peak should occur in the 12 groove data. When a polynomial fit was applied to the data for each flow, the angle of rotation appeared to be directly related to the vapor velocity.

In Fig. 8, the relation of film rotation to vapor velocity is evident. However, it appears that the rotation reaches a limiting condition at 12 grooves. The 12 and 20 groove tubes have essentially the same behavior. A relation between the film rotation, γ, and the gas velocity and number of grooves, n, was determined to be

$$\gamma(n, U_{sg}) = A_1(n)U_{sg} + B_1(n), \tag{4}$$

where

$$A_1 = 0.22n - 0.46, \tag{5}$$

$$B_1 = 4.67 - 3n. \tag{6}$$

The predictions based on this equation are plotted in Fig. 8 as solid lines.

While the data were well-correlated by the vapor velocity alone, it was found that including a liquid mass flow effect through the Froude rate was somewhat, though not dramatically, more effective [1].

4.7. Film thickness and the number of grooves

The effect of the number of grooves on the mean base film thickness is investigated through Fig. 6b. Similarly

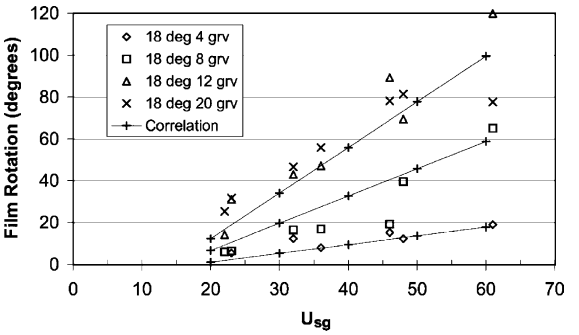

Fig. 8. Film rotation versus superficial gas velocity (U_{sg}) [m/s].

to the film thickness behavior with variation in helix angle, the base film is thicker in the grooved tubes for the lowest, stratified-annular flow condition. The remaining data, however, show that the grooves act in some manner to thin the base layer. No definite trend exists with respect to the number of grooves, but the 8 groove tube often generated the thinnest film. Inspection of the standard errors of the film thickness measurements indicated that the waviness of the film is increased in the 8 groove tube over that in the 20 groove and that the film thinning may be related to this increased surface activity.

At most of the flow conditions tested, the number of grooves appeared to have little effect on the flow distribution as displayed in Fig. 7b. At the lowest vapor flow rates for each of the two liquid flows, however, the distribution improves in the 20 groove tube by almost 50% over the smooth tube. In addition, the 0.006 kg/s, 0.42 quality data show that the distribution is directly related to the number of grooves.

4.8. Pressure drop

Fig. 9a plots the friction factors of the various tubes against the Lockhart–Martinelli parameter, X_{tt}. The Lockhart–Martinelli parameter was calculated according to

$$X_{tt} = \left(\frac{1-x}{x}\right)^{0.9}\left(\frac{\rho_g}{\rho_l}\right)^{0.5}\left(\frac{\mu_l}{\mu_g}\right)^{0.1}. \quad (7)$$

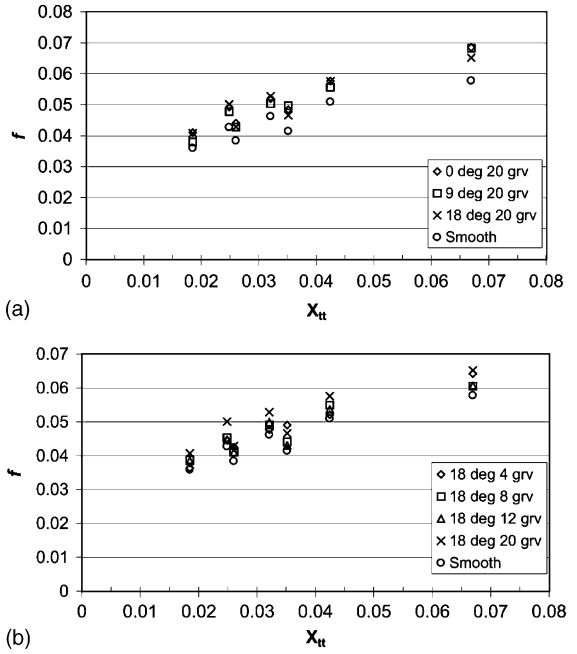

Fig. 9. Friction factor versus X_{tt} for tubes with different angles of grooves (a) and different numbers of grooves (b).

Clearly the presence of the grooves has only a minor effect on the pressure loss in the tubes. Groove angle appears to have only a small effect which is more pronounced in the higher liquid flow data. If the axial groove points are excluded, the friction factor is essentially directly proportional to the groove angle for three of the 0.006 kg/s flows. No clear pattern exists in the 0.003 kg/s data except at the lowest X_{tt} point where the pattern follows the 0.006 kg/s data. Pressure loss in the axial groove tube tends to coincide with the 18 degree data.

Although the effect is small, the friction factor is more directly related to groove number. As shown in Fig. 9b, frictional loss increases with groove number for all but two of the 0.003 kg/s data points. It is believed that at these two points where the 4 groove tube presents the highest friction factors, the results are influenced by a poorly formed joint in the test section. At these lowest flows, the vapor flow is sensitive to this gap between tubes and the pressure drop shows this. When the liquid flow is greater or more evenly distributed, the small gap is filled with liquid and the vapor flow is minimally affected.

5. Conclusion

The key findings of this work are:

- A relatively small number of grooves are necessary to redistribute the liquid film; this redistribution can be correlated with vapor phase velocity.
- No clear relationship was found between groove angle and film rotation.
- The grooves act in some manner so as to affect the stability of the liquid interface.
- The grooves can alter the flow such that lower mean film thickness values result.
- The pressure loss is directly related to the number of grooves in the tube, at least for these small numbers.

Acknowledgements

This work was supported by the Air Conditioning and Refrigeration Center at the University of Illinois at Urbana-Champaign, an NSF Industry-University Cooperative Research Center. Thanks to undergraduate research assistant Robert Shurig for his help in obtaining some of the film thickness data.

References

[1] T.A. Shedd, Characteristics of the liquid film in horizontal two-phase annular flow, Ph.D. thesis, University of Illinois at Urbana-Champaign, Urbana, IL, 2001.

[2] M. Ito, H. Kimura, Boiling heat transfer and pressure drop in internal spiral-grooved tubes, Bull. JSME 22 (171) (1979) 1251–1257.
[3] S.Y. Oh, A.E. Bergles, Experimental study of the effects of the spiral angle on evaporative heat transfer enhancement in microfin tubes, ASHRAE Trans. 104 (2) (1998) 1137–1143.
[4] H. Kimura, M. Ito, Evaporating heat transfer in horizontal internal spiral-grooved tubes in the region of low flow rates, Bull. JSME 24 (195) (1981) 1602–1607.
[5] S. Yoshida, T. Matsunaga, H.P. Hong, K. Nishikawa, Heat transfer enhancement in horizontal, spirally grooved evaporator tubes, JSME Int. J. 31 (3) (1988) 505–512.
[6] L.M. Chamra, R.L. Webb, M.R. Randlett, Advanced micro-fin tubes for evaporation, Int. J. Heat Mass Transfer 39 (9) (1996) 1827–1838.
[7] J.C. Khanpara, A.E. Bergles, M.B. Pate, Augmentation of R-113 in-tube evaporation with micro-fin tubes, ASHRAE Trans. 92 (2B) (1986) 506–524.
[8] L.M. Schlager, M.B. Pate, A.E. Bergles, Heat transfer and pressure drop during evaporation and condensation of R22 in horizontal micro-fin tubes, Int. J. Refrig. 12 (1989) 6–14.
[9] L.M. Schlager, M.B. Pate, A.E. Bergles, Evaporation and condensation heat transfer and pressure drop in horizontal, 12.7-mm microfin tubes with refrigerant 22, J. Heat Transfer—Trans. ASME 112 (1990) 1041–1047.
[10] L.M. Chamra, R.L. Webb, M.R. Randlett, Advanced micro-fin tubes for condensation, Int. J. Heat Mass Transfer 39 (9) (1996) 1839–1846.
[11] R. Chiang, Heat transfer and pressure drop during evaporation and condensation of refrigerant-22 in 7.5 mm and 10 mm diameter axial and helical grooved tubes, Heat Transfer—Atlanta 1993 89 (295) (1993) 205–210.
[12] Y. Shinohara, K. Oizumi, Y. Itoh, M. Hori, Heat-transfer tubes with grooved inner surface, U.S. Patent Number 4,658,892, ammended 1990 (1987).
[13] D. Graham, J.C. Chato, T.A. Newell, Heat transfer and pressure drop during condensation of Refrigerant 134a in an axially grooved tube, Int. J. Heat Mass Transfer 42 (11) (1999) 1935–1944.
[14] B.N. Taylor, C.E. Kuyatt, Guidelines for evaluating and expressing uncertainty of NIST measurement results, Tech. Rep. 1297, National Institute of Standards and Technology, Bethesda, MD, 1994.
[15] T.A. Shedd, T.A. Newell, Automated optical liquid film thickness measurement method, Rev. Sci. Instrum. 69 (12) (1998) 4205–4213.
[16] K.M. Plzak, T.A. Shedd, Verification of an optical liquid film thickness measurement system in horizontal annular two-phase flow, Experiments in Fluids, Submitted for publication.
[17] S. Jayanti, G.F. Hewitt, Hydrodynamics and heat transfer in wavy annular gas-liquid flow: a computational fluid dynamics study, Int. J. Heat Mass Transfer 40 (10) (1997) 2445–2460.